The glass-melting furnace and the crucibles of Südel (1723–1741, Switzerland): provenance of the raw materials and new evidence of high thermal performances

G. Eramo

Département de géosciences, minéralogie et pétrographie, université de Fribourg, 6, chemin-du-Musée, CH-1700 Fribourg, Switzerland

Abstract

Fifty crucible fragments and 10 fragments of the melting furnace of the forest glassworks of Südel (1723–1741, Ct. Luzern), were analyzed by petrographic, mineralogical and chemical techniques in order to assess the temperature reached in the melting chamber and to find out which raw materials were used to make the crucibles and the melting furnace. Since the crucibles were used in the melting furnace, the temperature estimations were based on both the crucibles and the refractory fragments, as they were parts of the same system. The temperature range in the melting chamber, estimated by the structural order of the new-formed cristobalite, points to a temperature range between 1350 and 1500 °C. However, three crucible samples recorded extreme temperatures as high as 1650 °C, suggesting very high flame temperatures for wood fuel. The analyzed red bricks were made with local calcium-poor clay. One of them was tempered with refractory fragments, demonstrating an in-house production and the recycling of such a material after its use. The crucibles and the refractory bricks were made with the same refractory clay. The former using unprocessed clay and the latter blending clay with chamotte. A comparison with Sidérolithique clayey sand samples from the Swiss Jura, shows strong affinities which may rule out the archaeological hypothesis of an exclusive provenance of such clays from Germany, suggesting an import from the Swiss Jura mountains.

Keywords: Forest glassworks; Glass technology; Refractory; Cristobalite; Switzerland; Pre-industrial period

1. Research aims

In the framework of the pre-industrial glass making in Europe, this study attempts to give some insight into the technological aspects of glass making in Switzerland in the early 18th century, by an archeometrical analysis of the glass-melting crucibles and of the fragments of the melting furnace of the forest glassworks of Südel (1723–1741). The aims of this paper are: (1) to determine the provenance of the raw materials of the melting furnace and the crucibles; (2) to verify the archaeological hypothesis of the in-house production of the red bricks and the refractory bricks of the melting furnace; (3) to understand the production technique of the bricks and crucibles and (4) to reconstruct the temperature distribution in the melting furnace.

E-mail address: giacomo.eramo@unifr.ch (G. Eramo).

2. Introduction

2.1. Glass production in Südel

The forest glassworks of Südel lies at ca. 20 km south-west from Luzern (Fig. 1) and is one of a dozen of glassworks active in the pre-industrial period (17th–19th century) in the Entlebuch region [2]. The glass production in the Entlebuch goes back to early 18th century when the first glassmakers' families, emigrated from the German Black Forest, installed their glassworks [3]. In the late Middle ages, due to the exhaustion of the wood supplies in the Black Forest, some wooded regions of Switzerland such as Entlebuch, Jura and Iberg attracted many glassmakers [4]. Wood ash was the main raw material used to produce glass and forced glassmakers to move their settlements each time the wood supply was exhausted. The glassworks of Südel was the first of a series of glassworks founded by the Siegwart family in the Entlebuch region [4] and produced bottles, drinking glasses, pharmaceutical glass and bull's eye

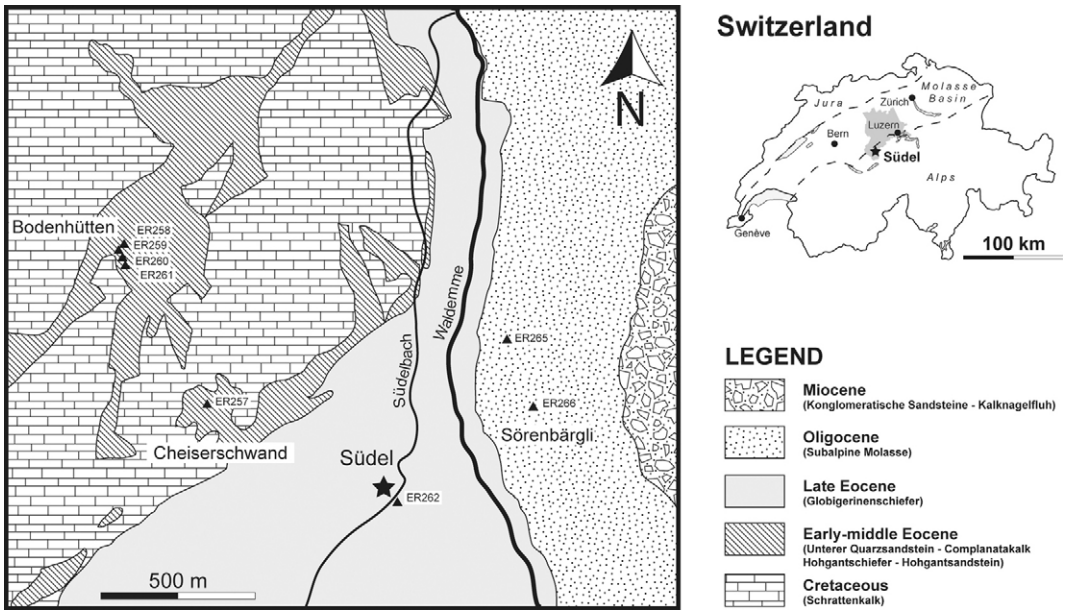

Fig. 1. Schematic geological map of Waldemme Valley after Schider [1] and position of the of raw materials samples. On the right. the map of Switzerland and location of Südel (shaded area = Ct. Luzern).

panes [5]. The vitreous finds consist almost exclusively of green glass with minor amounts of brown, blue and colorless fragments. Descoeudres et al. [5] reports a general potassium-calcium composition for this kind of glasses, characterized by a strong variation in CaO concentration (2.70–19.70 wt.%) and relative low K_2O (3.70–6.30 wt.%).

When the Südel glassworks was founded in 1723, 23 wagons with refractory earth and chamotte of unknown provenance were imported to produce the refractory bricks and the crucibles [3]. The term "*chamotte*" must probably be understood as clay fired at low temperature and used as a dehydrated component of the refractory clay. In the last year of activity (1741), a load of refractory earth and *chamotte* arrived from Germany [5]. It is also known that pure quartz sand (Hupper, Sidérolithique Formation) from Swiss Jura (Fig. 1) was used for the production of the colorless glass they used [2].

The archaeological excavations of the glassworks carried out by the "Denkmalpflege und Archäologie des Kantons Luzern" (1983/1984) brought to light the workshop area with the melting furnace (center) and the adjoining secondary furnaces, which were used to frit the raw materials to make the glass and to dry the wood fuel [5].

The furnace was formed by a central melting chamber and four "wings" which contained the annealing arches (Fig. 2). According to the typological classification of Horat [6], taking into account the entire plant, the melting furnace of Südel falls in the group of the "rectangular furnaces" (*Rechteckofen*, *Typ* A5). The overall length of the furnace was 9.2 m on the western and 9.8 m on the eastern side, with an overall width of 7.8 m on the northern and 7.4 m on the southern side. The dimensions of the melting chamber were 4.1 × 3.2 m. The two sieges were 80 cm high and their top surface was about 70 cm large. The central part of the sieges contained an air vent (8 × 20 cm) in order to increase the airflow rate in the fire

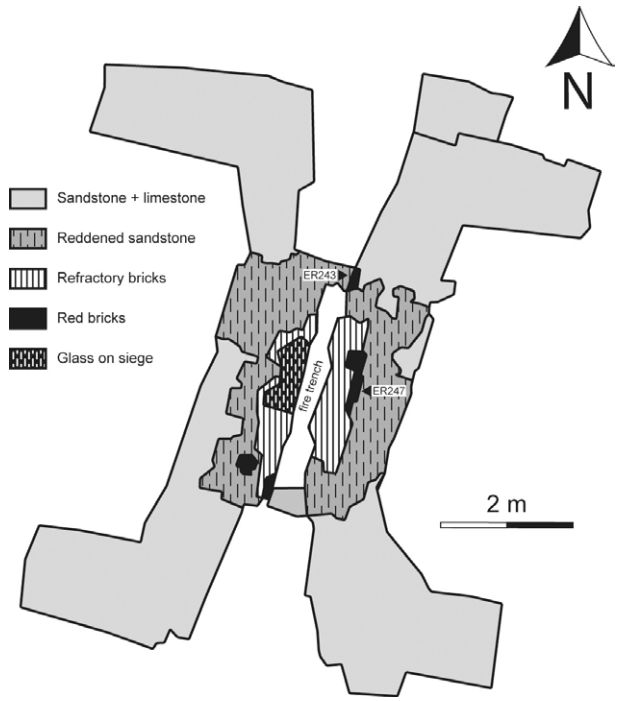

Fig. 2. Structural plan of the melting furnace after Descoeudres et al. [5] and position of the two red bricks analyzed in this study.

trench (Fig. 3). The melting chamber shows an inner and an outer structure made of different materials. The outer structure of the furnace was made of limestone and sandstone blocks bound with clay. The inner part of the melting chamber was made of red bricks and refractory bricks (Fig. 2) and the same clays of these bricks were used as binder [5]. No finds which could be clearly interpreted as part of the roof of the melting chamber were found.

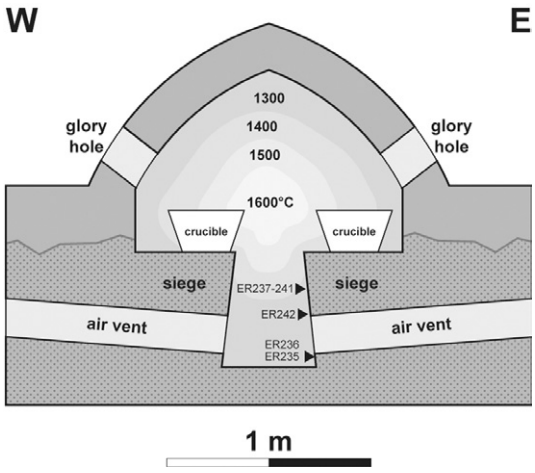

Fig. 3. Cross-section through the melting chamber according to Descoeudres et al. [5]. The dotted area represents the remains of the furnace. The positions of refractory brick samples are shown. The temperature distribution was inferred using cristobalite as archeothermometer. Temperatures above 1600 °C. recorded by three crucible fragments. may be due to the direct contact with the flame.

As concerns crucibles, many fragments were found in the workshop area. Fig. 4 shows the only restored crucible of Südel (bottom: 14 × 25 cm; rim: 26 × 42 cm; height: 33–36 cm), which could have contained about 35 kg of molten glass [5]. This oval shape was quite common in the 18th century [6–8]. The crucible is characterized by the orange color of the body and glass drippings on the side exposed to the wall of the melting chamber and by the grayish color and the fracture network on the side exposed to the flame (Fig. 4).

2.2. Geological setting

The Entlebuch region lies in the center of Switzerland, on the boundary between the Alpine Helvetic realm and the Subalpine Molasse [9]. The rocks cropping out in Waldemme Valley range from the Cretaceous Helvetic limestones up to the Neogene Molassic deposits (Fig. 1). Middle and late Eocene siliciclastic rocks, such as those of Klimsenhorn Formation and Hohgant Formation [10], are particularly suited for glass making purposes. Unterer Quarzsandstein and Complanatakalk (Klimsenhorn Formation), as well as Hohgant Quarzsandstein and Hohgant Schiefer (Hohgant Formation) crop out in a rather patchy manner on top of the Cretaceous limestones of the Schrattenfluh Mountain [1,10,11]. Globigerinenschiefer are present on the bottom of the valley constituting the substratum of Südel. Subalpine Molasse crop out on the eastern side of the valley. The Quaternary is represented by the moraine deposits covering the bottom of the valley and by the talus occurring on the eastern slope of the valley. The use of these local fine-grained Unterer Quarzsandstein and Hohgant Quarzsandstein as raw material for glass is historically known [2]. von Moos [12] argued that the weathered horizon of Hogant Quarzsandstein, instead of the original hard rock, was used by the glass makers of Südel as a glass batch component.

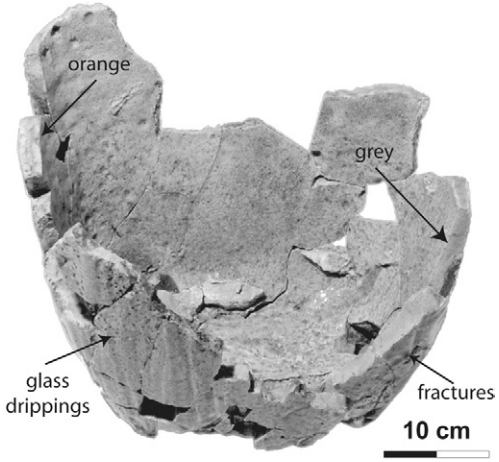

Fig. 4. Restored glass-melting crucible of the glassworks of Südel. Note the chromatic difference of the body and the wearing effects on the outer surface as consequence of its position in the melting chamber.

3. Sampling

3.1. Archaeological materials

Sixty fragments of the melting furnace and of the crucibles from the last level of utilization (1741) in the workshop area of the glassworks in Südel were sampled (Table 1).

The 50 crucible fragments were collected from different excavation units across the excavation area in order to avoid samples of the same object and samples with different thickness and different positions with respect to the crucible body were chosen (Table 1).

The eight fragments of refractory bricks belong to the siege on the eastern side of the furnace. The fragments represent different positions, from the bottom to the top of the fire trench (Fig. 3). From the same siege, a red brick, originally positioned in the core of the structure, and another from the northern aperture of the fire trench, exposed to the flame, were also collected (Fig. 2). The original position of these furnace fragments is well documented by the archaeologists.

3.2. Raw materials

Sampling of the local clays was made after the petrographic, mineralogical and chemical characterization of the archaeological objects (Table 2). Sandstones as well as unconsolidated sediments which could have been used as raw materials for the melting furnace and the crucibles were sampled. Together with the sandstone samples, some specimens from the alteration surface were collected as well (ER259 and 261) to investigate the reciprocal chemical and petrographic differences.

4. Experimental

4.1. Petrographic analysis

All the archaeological samples and the sandstones were analyzed under a “Carl Zeiss Standard” polarizing microscope.

Table 1
The analyzed samples of the glassworks of Südel

Sample	Type	Color	Petrographic group	Phase content	Temper	Crs $d_{(101)}$
ER185	Crucible(rim)	Gray	A	Crs + Qm* + Mul	Chamotte	4.062
ER186	Crucible(rim)	Gray	A	Crs + Qm* + Mul		4.059
ER187	Crucible(wall)	Gray-rose	A	Crs + Qm* + Mul		4.059
ER188	Crucible(rim)	Gray	A	Crs + Qm* + Mul		4.059
ER189	Crucible(rim)	Dark rose	A	Qm* + Crs + Mul + (Trd)		4.059
ER190	Crucible(wall)	Dark rose	A	Qm* + Crs + Mul + (Trd)		4.060
ER191	Crucible(wall)	Dark rose	A	Qm* + Crs + Mul + (Trd)		4.059
ER192	Crucible(wall)	Gray	A	Crs + Qm* + Mul		4.059
ER193	Crucible(rim)	Gray	A	Crs + Qm* + Mul		4.062
ER194	Crucible(wall)	Gray	A	Qm* + Crs + Mul + (Trd)		4.059
ER195	Crucible(rim)	Gray	A	Crs + Qm* + Mul		4.061
ER196	Crucible(wall)	Pale beige	A	Crs + Qm* + Mul		4.066
ER197	Crucible(rim)	Dark rose	A	Qm* + Crs + Mul + (Trd)		4.059
ER198	Crucible(wall)	Gray–violet	A	Crs + Qm* + Mul	Chamotte	4.054
ER199	Crucible(wall)	Gray	A	Crs + Qm* + Mul		4.063
ER200	Crucible(wall)	Zoned: white–yelllow	A	Qm* + Crs + Mul + (Trd)		4.062
ER201	Crucible(wall)	Zoned: white–yelllow	A	Qm* + Crs + Mul + (Trd)		4.064
ER202	Crucible(wall)	Gray	A	Crs + Qm* + Mul		4.059
ER203	Crucible(rim)	Pale yellow	A	Qm* + Crs + Mul + (Trd)		4.059
ER204	Crucible(rim)	Pale yellow	A	Qm* + Crs + Mul + (Trd)		4.064
ER205	Crucible(wall)	Pale yellow	A	Qm* + Crs + Mul + (Trd)		4.059
ER206	Crucible(rim)	Dark orange	A	Qm* + Crs + Mul + (Trd)		4.059
ER207	Crucible(wall)	Gray	A	Qm* + Crs + Mul + (Trd)		4.059
ER208	Crucible(rim)	Gray	A	Qm* + Crs + Mul + (Trd)		4.062
ER209	Crucible(rim)	Yellow–orange	A	Crs + Qm* + Mul		4.060
ER210	Crucible(rim)	Yellow–orange	A	Crs + Qm* + Mul		4.059
ER211	Crucible(wall)	Pale gray	A	Crs + Qm* + Mul		4.062
ER212	Crucible(wall)	Orange–gray	A	Crs + Qm* + Mul		4.062
ER213	Crucible(bottom)	Gray	A	Qm* + Crs + Mul + (Trd)		4.059
ER214	Crucible(bottom)	Dark orange	A	Qm* + Crs + Mul + (Trd)		4.059
ER215	Crucible(wall)	Gray	A	Crs + Qm* + Mul		4.059
ER216	Crucible(rim)	Yellow	A	Qm* + Crs + Mul + (Trd)		4.059
ER217	Crucible(wall)	Yellow	A	Qm* + Crs + Mul + (Trd)		4.059
ER218	Crucible(rim)	Pale gray	A	Crs + Qm* + Mul		4.062
ER219	Crucible(wall)	Pale gray	A	Qm* + Crs + Mul + (Trd)		4.059
ER220	Crucible(bottom)	Gray	A	Qm* + Crs + Mul + (Trd)		4.053
ER221	Crucible(wall)	Gray	A	Crs + Qm* + Mul		4.062
ER222	Crucible(wall)	Gray	A	Crs + Qm* + Mul		4.062
ER223	Crucible(wall)	Gray	A	Crs + Qm* + Mul		4.059
ER224	Crucible(rim)	Pale gray	A	Qm* + Crs + Mul + (Trd)		4.059
ER225	Crucible(wall)	Pale gray	A	Crs + Qm* + Mul		4.059
ER226	Crucible(bottom)	Gray	A	Qm* + Crs + Mul + (Trd)		4.059
ER227	Crucible(wall)	Gray	A	Qm* + Crs + Mul + (Trd)		4.059
ER228	Crucible(wall)	Pale yellow	A	Qm* + Crs + Mul + (Trd)		4.063
ER229	Crucible(wall)	Pale gray	A	Qm* + Crs + Mul + (Trd)		4.059
ER230	Crucible(wall)	Pale yellow	A	Qm* + Crs + Mul + (Trd)		4.063
ER231	Crucible(bottom)	Pale yellow	A	Qm* + Crs + Mul + (Trd)		4.059
ER232	Crucible(wall)	Pale gray	A	Qm* + Crs + Mul + (Trd)		4.066
ER233	Crucible(wall)	Gray	A	Crs + Qm* + Mul		4.063
ER234	Crucible(rim)	Gray	A	Qm* + Crs + Mul + (Trd)	Chamotte	4.055
ER235	Refractory brick (with fritted ash)	Yellow	A	Qm* + Crs + Mul	Chamotte	4.077
ER236	Refractory brick (with fritted ash)	Yellow	A	Qm* + Crs + Mul	Chamotte	4.078
ER237	Refractory brick	Yellow	A	Qm* + Crs + Mul + (Trd)	Chamotte	4.067
ER238	Refractory brick	Yellow	A	Qm* + Crs + Mul + (Trd)	Chamotte	4.066
ER239	Refractory brick	Yellow	A	Qm* + Crs + Mul + Trd	Chamotte	4.064
ER240	Refractory brick	Yellow	A	Qm* + Crs + Mul + Trd	Chamotte	4.066
ER241	Refractory brick	Yellow	A	Qm* + Crs + Mul + (Trd)	Chamotte	4.073
ER242	Refractory brick (upon air vent)	Yellow	A	Qm* + Crs + Mul + (Trd)	Chamotte	4.072
ER243	Red brick (partially molten)	Zoned: violet–orange	B	Qm* + Qp* + (Hem) + (Pl)	Recycled refractory	
ER247	Red brick	Marbled fabric	C	Qm* + Ill/Mus* + (Pl)		

Mineral abbreviations: Ill/Mus: illite/muscovite; Mul: mullite; Pl: plagioclase; Qm: monocrystalline quartz; Qp: polycrystalline quartz; Hem: hematite; cristobalite; Crs: cristobalite; Trd: tridymite.

Table 2
The analyzed raw materials from the Waldemme Valley

Sample	Locality	Coordinates	Lithology	Formation	Age	Mineralogy	Cement	Fossils
ER257	Cheiserschwand	642.650/187.500	Sandstone (ms)	Complanatakalk	Eocene	Qm, Qp, Kfs, Glt	Micrite	Nummulites, bivalves, algae
ER258	Bodenhütten	642.250/188.375	Sandstone (ms)	Unterer quarzsandstein	Eocene	Qm, Qp, Kfs, Ms, Glt (Zrn)	Silica	
ER259	Bodenhütten	642.250/188.375	Sand (ms)	Unterer quarzsandstein	Eocene	Qm		
ER260	Bodenhütten	642.375/188.375	Sandstone (vfs)	Unterer quarzsandstein	Eocene	Qm, Kfs, Ill/Ms, Glt (Zrn)	Micrite	Foraminifera
ER261	Bodenhütten	642.375/188.375	Sand (vfs)	Unterer quarzsandstein	Eocene	Qm, Kfs, Ill/Ms, Kln		
ER262	Südel	643.600/187.075	Clay	Moraine	Quaternary	Qm, Cal, Kln, Pl, Ill/Ms		
ER265	Sörenbärgli	644.125/187.925	Clay	Talus	Quaternary	Qm, Pl, Ill/Ms		
ER266	Sörenbärgli	644.175/187.500	Clay	Talus	Quaternary	Qm, Pl, Ill/Ms		

Grain-size abbreviations: ms: medium sand; vfs: very fine sand. Mineral abbreviations: Cal: calcite; Glt: glauconite; Kfs: K-feldspar; Ill/Mus: illite/muscovite; Mul: mullite; Pl: plagioclase; Qm: monocrystalline quartz; Qp: polycrystalline quartz; Zrn: zircon; Kln: kaolinite. Minor phases in parentheses.

4.2. Grain-size analysis in thin section

Fifty thin sections of crucibles and eight thin sections of the refractory fragments of the melting furnace were analyzed. A Swift & Sons point-counter, mounted on the petrographic microscope, was used (1/3 of mm as line distance and as lateral step). The maximum apparent diameter of grains was measured with the aid of a micrometer eyepiece at ×10 magnification. Six size classes were distinguished: < 63, 63–125, 125–250, 250–500, 500–1000 and 1000–2000 μm. Between 500 and 600 points per thin section were counted as the minimum number of counts necessary for routine analyses [13]. Grain-sizes data were reported in φ values (Table 3) and represented by cumulative frequency curves (Fig. 5).

4.3. X-ray diffraction (XRD)

The mineral composition was determined by XRD analyses carried out on a Philips PW1800 diffractometer with Cu–K_α radiation at 40 kV and 40 mA (step angle of 0.02°, 2θ from 2° to 65°, measuring time 1 s per step).

4.4. Loss on ignition (LOI)

Three grams of dry powdered sample were calcined at 1000 °C for 1 hour and were weighed to determine the LOI.

4.5. X-ray fluorescence (XRF)

Analyses were carried out on glassy tablets, which were prepared by melting 0.700 g of calcined samples, 0.350 g of Li fluoride and 6.650 g of Li tetraborate at 1150 °C in a Pt crucible. Bulk chemical analyses for major and trace elements were performed by a Philips PW 2400 XRF spectrometer equipped with a rhodium X-ray tube. Since the standards used do not cover the very high percentages of SiO_2 in the samples, deviations up to 4 wt.% from the 100 wt.% occur (Tables 4 and 5).

4.6. Principal component analysis (PCA)

It was carried out on a dataset which comprised 142 samples (Südel: 50 crucibles, eight refractories; Derrière Sairoche: 43 crucibles, 22 refractories; raw materials: 19 Hupper), using 15 chemical and grain-size variables which have few missing values and higher variance. The "<0.01" in the data set were approximated to 0.01. Since the variables (SiO_2, TiO_2, Al_2O_3, Fe_2O_{3tot}, MgO, CaO, K_2O, Cr, Sr, Zr, –1–0φ, 1–2φ, 2–3φ, 3–4φ and >4φ) used for the PCA are expressed in different units, standardization was necessary to ensure a similar order of magnitude and variance.

5. Results

In the following paragraphs, the petrographic (Tables 1–3) as well as the chemical analyses (Tables 4 and 5) of the archaeological objects and of the local raw materials were reported.

5.1. Archaeological materials

5.1.1. Crucibles and refractory bricks (petrographic group A)

The crucible's body shows colors going from yellow, orange to gray and violet, whereas the refractory bricks are yellow (Table 1).

In thin section, the refractory bricks and the crucibles show a very homogeneous fabric and petrographic composition. The non-plastic component consists exclusively of monocrystalline quartz (Fig. 6). The grains coarser than silt are more rounded and fractured.

The coarsest grain diameters range from 0.4 to 1.5 mm for the crucibles and from 1.4 to 2.8 mm for the refractory bricks. The latter show frequent *chamotte* inclusions with a sharp boundary, an angular shape and a fine grained fabric (Fig. 7). Rare fragments of *chamotte* with the same features were also observed in only three crucible samples (ER 185, 189 and 234).

Fig. 5 shows the grain-size distribution of the crucibles and the refractory bricks measured in thin section. The grain-size distribution shows that the 3–4φ size class is prevalent, although the refractory bricks contain higher percentages of coarse sand (<–1φ, −1−0φ and 0–1φ). Data dispersion increases going from the coarse to the fine classes (Table 3).

Only SiO_2 and Al_2O_3 and TiO_2 exceed 1 wt.% in the bulk chemical composition of the samples, whereas Zr, Sr and Cr are the most abundant trace elements.

Table 3
Grain-size data (vol.%) of the crucibles and the refractory bricks obtained by point counting in thin section

	φ	<–1	–1–0	0–1	1–2	2–3	3–4	>4
	(μm)	*f*>2000	1000–2000	500–1000	250–500	125–250	63–125	*f*< 63
Crucibles	ER185	0.0	0.0	3.2	5.4	14.7	21.1	55.6
	ER186	0.0	0.2	0.9	5.3	19.5	17.4	56.7
	ER187	0.0	0.0	1.4	7.2	17.5	23.2	50.8
	ER188	0.0	0.0	3.2	7.7	21.0	20.5	47.6
	ER189	0.0	0.6	7.0	6.4	20.6	31.0	34.4
	ER190	0.0	1.8	5.1	7.1	22.7	30.8	32.4
	ER191	0.0	0.3	3.9	6.0	16.2	24.4	49.1
	ER192	0.0	0.0	1.6	4.0	19.7	27.1	47.5
	ER193	0.0	0.0	0.7	3.7	16.0	29.9	49.6
	ER194	0.0	0.0	0.5	2.7	16.1	36.0	44.7
	ER195	0.0	0.2	0.8	5.1	22.0	24.4	47.5
	ER196	0.0	0.0	1.4	3.8	18.0	34.8	41.9
	ER197	0.0	0.0	5.2	6.1	20.0	30.6	38.0
	ER198	0.0	0.6	2.0	4.2	21.1	32.5	39.6
	ER199	0.0	0.2	1.4	2.7	20.8	31.1	43.9
	ER200	0.0	0.0	1.8	4.6	18.7	32.6	42.2
	ER201	0.0	0.0	0.9	2.1	17.6	32.9	46.5
	ER202	0.0	0.0	0.9	4.3	17.4	30.7	46.7
	ER203	0.0	0.0	1.1	5.2	20.5	29.8	43.5
	ER204	0.0	0.0	2.4	5.4	18.4	26.6	47.2
	ER205	0.0	0.0	1.3	5.1	19.3	31.2	43.1
	ER206	0.0	0.0	1.1	3.6	20.7	29.2	45.4
	ER207	0.0	0.0	0.7	2.2	17.4	31.3	48.5
	ER208	0.0	0.0	0.4	2.5	16.4	26.7	54.0
	ER209	0.0	0.0	0.7	3.5	17.6	24.9	53.4
	ER210	0.0	0.0	0.6	3.4	16.8	26.5	52.7
	ER211	0.0	0.2	0.2	2.2	14.2	28.7	54.7
	ER212	0.0	0.0	0.9	4.3	14.6	31.3	48.9
	ER213	0.0	0.0	0.2	4.3	18.3	33.9	43.3
	ER214	0.0	0.0	0.8	4.4	12.8	31.0	51.0
	ER215	0.0	0.0	0.7	6.5	15.4	27.8	49.7
	ER216	0.0	0.0	0.5	4.5	14.7	29.9	50.3
	ER217	0.0	0.5	1.2	2.2	12.4	33.2	50.5
	ER218	0.0	0.2	0.6	1.9	15.0	31.2	51.1
	ER219	0.0	0.2	2.7	5.8	15.9	25.8	49.6
	ER220	0.0	0.3	1.1	7.2	18.2	26.6	46.6
	ER221	0.0	0.0	1.9	2.5	14.0	25.0	56.5
	ER222	0.0	0.0	2.1	4.1	17.2	23.1	53.5
	ER223	0.0	0.0	1.0	3.5	16.3	20.2	59.1
	ER224	0.0	0.0	1.0	3.5	15.6	27.5	52.5
	ER225	0.0	0.8	1.6	4.0	13.6	31.2	48.8
	ER226	0.0	0.0	2.0	4.4	17.1	29.5	47.0
	ER227	0.0	0.0	0.5	4.5	16.9	29.2	48.8
	ER228	0.0	0.0	1.5	4.4	17.1	33.2	43.8
	ER229	0.0	0.4	0.4	4.3	21.5	30.7	42.7
	ER230	0.0	0.0	0.5	2.8	18.8	31.3	46.6
	ER231	0.0	0.0	0.0	2.5	15.4	36.8	45.2
	ER232	0.0	0.0	1.8	3.9	15.2	34.0	45.1
	ER233	0.0	0.0	0.7	2.3	14.2	40.4	42.5
	ER234	0.0	0.0	0.0	4.0	16.7	35.3	44.0
	mean	0.0	0.1	1.5	4.3	17.4	29.3	47.5
	σ	0.0	0.3	1.4	1.5	2.5	4.6	5.4
Refractory bricks	ER235	0.0	1.3	3.4	4.8	18.7	30.0	41.7
	ER236	0.0	1.2	2.2	2.8	19.2	38.0	36.6
	ER237	0.0	3.6	3.8	2.0	13.6	31.0	46.0
	ER238	0.0	2.9	3.8	2.0	12.3	28.6	50.4
	ER239	0.0	1.5	2.9	3.8	15.3	29.6	46.9
	ER240	0.0	3.8	2.8	2.8	15.4	33.6	41.6
	ER241	2.7	1.1	1.3	4.5	14.3	35.8	40.3
	ER242	0.0	1.5	1.1	2.7	11.6	36.3	46.8
	mean	0.3	2.1	2.7	3.2	15.1	32.9	43.8
	σ	1.0	1.1	1.1	1.1	2.7	3.5	4.5

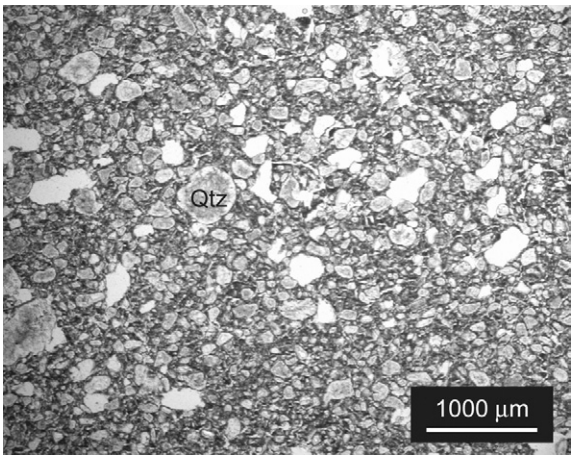

Fig. 5. Cumulative frequency ranges of the crucibles ($n = 50$) and of the refractory bricks ($n = 8$) of Südel. The grain-size distribution of the refractory bricks matches that of the crucibles.

5.1.2. Red brick (petrographic group B)

The iron-rich matrix gives the red color to the sample ER243. The matrix is low birefringent and homogeneous and still contains few amounts of illite/muscovite and hematite. The non-plastic fraction is formed by fine quartz sand and coarse crucible clasts recycled as temper (max. diam. 6.7 mm) (Fig. 8). Few amounts of cristobalite and mullite were detected by XRD.

5.1.3. Red brick with marbled fabric (petrographic group C)

The non-plastic fraction is composed almost exclusively of monocrystalline quartz (max. diam. 1.1 mm). It constitutes about 60% in volume of the sample (Fig. 9). The matrix has a medium birefringence and a marbled structure probably due to a bad mixing of two original clays or of a heterogeneous one. Few quantities of illite/muscovite are present. ER247 is richer than ER243 in Fe_2O_{3tot}, Na_2O and K_2O, while only Ba and Zr exceed the 100 ppm among the trace elements.

5.2. Local raw materials

The petrographic features of the three sandstones observed in thin section are summarized in Table 2. Monocrystalline quartz is the prevalent clastic component, while polycrystalline quartz occurs only in small amounts or is even absent (ER260). Few quantities of potassium feldspar, muscovite and glauconite occur in every sample. As for accessory minerals, only zircon was detected. ER257 and 260 have micritic cement, whilst ER258 has silica cement (Fig. 10). In ER260, the clastic portion is finer than in the other two cases. Bioclasts of nummulites, bivalves and red algae are present in ER257 (Fig. 11) and of foraminifera in ER260 (Fig. 12).

The weathering products of Unterer Quarzsandstein (ER259 and 261) are richer in quartz than their parent rock. They differ in their clay and the potassium feldspar content (Table 2). Both weathering products and the quaternary talus clays (ER265 and 266) have CaO less than 1 wt.%.

Contrasting, the moraine sample ER262 is a calcareous clay with quartz and plagioclase clasts.

6. Discussion

6.1. Raw materials

6.1.1. Petrographic group A

Petrographic analyses of the archaeological materials reveal the use of at least two CaO-poor clayey raw materials. The first is supposed to have been composed of quartz sand and kaolinitic clay, used for the crucibles and the refractory bricks, while the second was an illitic clay more or less rich in iron-oxides and -hydroxides, used for the red bricks. The moraine clay ER262 close to the glassworks of Südel can not be the clay source, because of its high calcite content. The high calcite content of ER257 (Complanatakalk) is incompatible with the temper and the non-plastic inclusions of the analyzed archaeological materials. The mineralogical difference between the samples of Unterer Quarzsandstein (ER258 and 260) and their weathering products (ER259 and 261) reveals the dissolution and the leaching of calcite and the mobilization of clay minerals, respectively. Although these results demonstrate that it was possible to exploit in loco calcite-free sands from calcite-cemented sandstone (ER260), the higher concentration of alkali and alkaline earth oxides and trace elements (Ba and Rb) of the weathering products compared to that of petrographic group A excludes their use as refractory earth.

However, the chemical composition of the weathering products of Unterer Quarzsandstein is similar to those of two analyzed sand samples found in the workshop area reported by Descoeudres et al. [5] and which are supposed to be the raw material for the glass.

6.1.2. Petrographic group B and C

The red bricks show mineralogical (illite/muscovite) and chemical (low CaO percentages) similarities with the clays from the talus on the eastern side of the Waldemme Valley. The absence of illite/muscovite in ER243 is due to firing (see below). Both two red bricks have different fabrics, but close chemical composition, which could be explained by different processing of the same heterogeneous clay. In fact, red brick ER243 was tempered with recycled crucible fragments and coarse sand, while ER247 shows no tempering. Therefore, the local provenance of raw material as well as the in-house production of the red bricks (petrographic group B and C) can be confirmed. On the contrary, the compositional incompatibility (Ba and Rb) of the local raw materials with the refractory and crucible fragments confirms the historical information of foreign provenance of the refractory clay at least for the last period of activity of the glassworks.

6.1.3. Which refractory clay for Südel?

The petrographic observations showed that only rare fragments of *chamotte* are present in the crucible body (ER185, 189 and 234), while they are very common in the refractory

Table 4
Major oxides and trace element concentrations (XRF) of the archaeological samples (LOI=loss on ignition)

		SiO_2	TiO_2	Al_2O_3	Fe_2O_{3tot}	MnO	MgO	CaO	Na_2O	K_2O	P_2O_5	SUM	LOI	Ba	Cr	Cu	Nb	Ni	Pb	Rb	Sr	Y	Zn	Zr
	Sample	(wt.%)	(wt.%)	(wt.%)	(wt.%)	(wt.%)	(wt.%)	(wt.%)	(wt.%)	(wt.%)	(wt.%)	(wt.%)	(wt.%)	(ppm)	(ppm)	(ppm)	(ppm)	(ppm)	(ppm)	(ppm)	(ppm)	(ppm)	(ppm)	(ppm)
Crucibles	ER185	88.73	1.04	8.28	0.49	< 0.01	0.06	0.15	< 0.01	0.10	0.03	98.94	0.08	< 12	49	< 2	18	13	11	< 3	85	20	5	389
	ER186	86.70	1.21	9.41	0.57	< 0.01	0.07	0.16	< 0.01	0.15	0.05	98.39	0.06	31	58	< 2	23	13	18	< 3	86	21	8	415
	ER187	86.89	1.20	9.43	0.56	< 0.01	0.06	0.17	< 0.01	0.13	0.05	98.55	0.07	< 12	54	< 2	22	14	19	< 3	86	20	8	408
	ER188	89.43	1.03	8.28	0.49	< 0.01	0.06	0.14	0.04	0.11	0.04	99.69	0.06	< 12	47	3	20	16	7	< 3	85	20	3	386
	ER189	88.95	1.06	7.87	0.50	< 0.01	0.07	0.16	< 0.01	0.23	0.05	98.95	0.09	< 12	46	< 2	20	10	8	< 3	95	19	3	387
	ER190	88.55	1.03	7.49	0.42	< 0.01	0.06	0.14	< 0.01	0.44	0.04	98.22	0.07	< 12	51	< 2	19	3	< 7	< 3	103	20	3	368
	ER191	88.15	1.05	7.75	0.49	< 0.01	0.07	0.16	< 0.01	0.19	0.04	97.96	0.08	< 12	53	< 2	20	8	< 7	< 3	91	20	2	369
	ER 192	87.31	1.02	8.06	0.49	< 0.01	0.07	0.14	0.04	0.11	0.02	97.32	0.08	< 12	42	< 2	18	13	12	< 3	84	20	6	377
	ER 193	85.64	1.21	9.37	0.56	< 0.01	0.06	0.17	0.23	0.16	0.03	97.51	0.11	16	61	7	22	13	19	< 3	84	21	7	390
	ER 194	87.03	1.24	8.87	0.56	< 0.01	0.06	0.17	0.04	0.32	0.04	98.46	0.10	< 12	61	434	23	6	8	4	124	20	2	411
	ER 195	86.23	1.20	9.40	0.56	< 0.01	0.06	0.16	< 0.01	0.15	0.04	97.87	0.07	< 12	59	3	23	13	15	< 3	85	20	8	402
	ER 196	85.84	1.20	9.33	0.55	< 0.01	0.07	0.15	< 0.01	0.14	0.04	97.40	0.08	18	59	91	23	14	17	< 3	86	22	9	401
	ER 197	88.13	1.05	7.81	0.51	< 0.01	0.06	0.16	< 0.01	0.24	0.03	98.06	0.09	13	45	< 2	20	10	< 7	5	92	19	2	364
	ER 198	88.30	1.03	8.23	0.49	< 0.01	0.06	0.15	< 0.01	0.10	0.03	98.45	0.06	< 12	45	< 2	21	12	14	7	84	19	< 2	387
	ER 199	87.15	1.21	9.48	0.57	< 0.01	0.07	0.17	< 0.01	0.13	0.04	98.89	0.07	28	59	< 2	22	15	18	9	84	20	8	408
	ER 200	89.19	1.12	8.47	0.43	< 0.01	0.06	0.11	< 0.01	0.16	0.03	99.71	0.10	22	55	759	22	10	< 7	9	76	17	< 2	393
	ER 201	88.55	1.12	8.36	0.42	< 0.01	0.06	0.11	< 0.01	0.16	0.03	98.87	0.08	< 12	51	< 2	22	10	< 7	7	76	18	< 2	378
	ER 202	88.37	1.12	9.16	0.49	0.01	0.07	0.18	< 0.01	0.16	0.03	99.66	0.14	< 12	55	< 2	21	15	12	8	67	19	< 2	386
	ER 203	89.27	1.01	7.59	0.28	< 0.01	0.06	0.20	0.10	0.76	0.03	99.35	0.18	< 12	53	< 2	18	3	< 7	21	73	16	< 2	370
	ER 204	85.83	1.01	7.29	0.29	< 0.01	0.06	0.20	0.07	0.61	0.03	95.46	0.18	18	52	39	20	5	< 7	19	74	18	< 2	377
	ER 205	89.43	1.01	7.57	0.30	< 0.01	0.06	0.20	0.11	0.55	0.03	99.32	0.17	< 12	48	23	19	< 3	< 7	18	74	16	< 2	365
	ER 206	84.54	1.32	11.60	0.70	< 0.01	0.07	0.30	0.22	0.24	0.04	99.11	0.06	17	81	< 2	25	14	12	< 3	89	21	5	391
	ER 207	86.67	1.21	8.93	0.62	< 0.01	0.07	0.21	< 0.01	0.18	0.04	98.00	0.12	49	58	< 2	22	14	11	< 3	122	22	5	418
	ER 208	87.32	1.21	9.01	0.63	< 0.01	0.09	0.27	< 0.01	0.25	0.04	98.89	0.14	< 12	60	< 2	23	9	7	< 3	120	21	4	424
	ER 209	84.31	1.32	11.38	0.77	< 0.01	0.05	0.71	< 0.01	0.16	0.04	98.81	0.08	< 12	78	< 2	25	16	14	< 3	97	21	4	401
	ER 210	83.43	1.31	11.38	0.76	< 0.01	0.06	0.86	< 0.01	0.45	0.05	98.37	0.13	18	83	43	25	8	10	< 3	96	21	5	383
	ER 211	87.34	1.24	9.00	0.56	< 0.01	0.06	0.20	< 0.01	0.23	0.04	98.74	0.18	34	60	< 2	24	9	< 7	< 3	111	21	5	410
	ER 212	87.35	1.20	8.71	0.59	< 0.01	0.06	0.12	< 0.01	0.09	0.04	98.23	0.13	33	53	< 2	23	14	17	< 3	101	20	6	422
	ER 213	89.01	0.97	7.57	0.40	< 0.01	0.05	0.08	0.02	0.14	0.02	98.34	0.10	24	38	< 2	18	8	< 7	< 3	67	18	< 2	359
	ER 214	87.99	1.06	8.24	0.45	< 0.01	0.06	0.12	< 0.01	0.18	0.03	98.19	0.08	< 12	47	< 2	21	6	< 7	< 3	77	20	< 2	386
	ER 215	86.52	1.23	10.87	0.61	< 0.01	0.06	0.20	< 0.01	0.16	0.04	99.77	0.08	26	67	20	23	14	17	< 3	89	21	10	403
	ER 216	85.64	1.15	9.87	0.58	< 0.01	0.06	0.23	0.05	0.29	0.04	97.99	0.13	< 12	60	< 2	22	11	9	< 3	90	20	4	388

(continued)

Table 4 *(continued)*

		SiO_2	TiO_2	Al_2O_3	Fe_2O_{3tot}	MnO	MgO	CaO	Na_2O	K_2O	P_2O_5	SUM	LOI	Ba	Cr	Cu	Nb	Ni	Pb	Rb	Sr	Y	Zn	Zr
	Sample	(wt.%)	(wt.%)	(wt.%)	(wt.%)	(wt.%)	(wt.%)	(wt.%)	(wt.%)	(wt.%)	(wt.%)	(wt.%)	(wt.%)	(ppm)	(ppm)	(ppm)	(ppm)	(ppm)	(ppm)	(ppm)	(ppm)	(ppm)	(ppm)	(ppm)
	ER 217	86.11	1.15	9.83	0.59	< 0.01	0.06	0.24	< 0.01	0.27	0.04	98.38	0.13	< 12	65	218	23	10	< 7	< 3	91	20	5	398
	ER 218	85.25	1.23	10.64	0.62	0.01	0.07	0.31	< 0.01	0.18	0.06	98.44	0.11	15	68	< 2	23	15	13	< 3	87	20	9	400
	ER 219	88.38	0.92	7.45	0.38	< 0.01	0.07	0.22	0.32	0.39	0.03	98.20	0.10	< 12	41	< 2	18	5	< 7	< 3	63	18	< 2	346
	ER 220	87.07	0.96	8.91	0.42	< 0.01	0.07	0.17	0.24	0.20	0.03	98.14	0.18	< 12	51	< 2	19	11	< 7	< 3	61	20	< 2	354
	ER 221	83.63	1.35	11.29	0.78	< 0.01	0.06	0.69	< 0.01	0.21	0.05	98.13	0.07	< 12	75	< 2	25	14	9	< 3	102	23	6	396
	ER 222	88.79	0.99	8.13	0.44	< 0.01	0.06	0.18	< 0.01	0.10	0.03	98.78	0.11	< 12	47	< 2	20	12	12	< 3	65	19	4	374
	ER 223	83.70	1.35	11.28	0.78	< 0.01	0.06	0.68	0.01	0.24	0.06	98.23	0.16	30	78	< 2	24	11	< 7	< 3	101	22	4	389
	ER 224	85.90	1.15	10.02	0.53	< 0.01	0.15	0.29	0.86	0.38	0.04	99.39	0.17	< 12	67	30	23	18	12	< 3	72	19	7	382
	ER 225	86.79	1.00	9.58	0.52	< 0.01	0.12	0.20	< 0.01	0.31	0.05	98.66	0.25	41	65	< 2	18	13	23	11	73	20	5	357
	ER 226	87.81	0.95	8.86	0.42	< 0.01	0.07	0.16	0.17	0.20	0.04	98.73	0.18	< 12	52	< 2	18	11	< 7	< 3	61	18	< 2	354
	ER 227	81.45	0.85	13.97	0.80	< 0.01	0.08	0.26	< 0.01	0.34	0.03	97.84	0.13	< 12	86	< 2	18	20	10	6	53	21	4	299
	ER 228	86.54	1.10	8.65	0.37	< 0.01	0.06	0.18	< 0.01	0.76	0.04	97.76	0.24	< 12	55	< 2	22	< 3	< 7	10	86	20	< 2	380
	ER 229	87.66	0.95	8.83	0.41	< 0.01	0.07	0.17	0.03	0.27	0.03	98.49	0.19	< 12	50	< 2	17	5	< 7	< 3	60	19	< 2	350
	ER 230	83.65	1.29	11.76	0.78	< 0.01	0.06	0.34	0.37	0.40	0.07	98.79	0.14	< 12	74	< 2	25	8	< 7	< 3	94	22	4	376
	ER 231	87.67	1.15	8.62	0.45	< 0.01	0.06	0.10	< 0.01	0.22	0.03	98.37	0.17	< 12	52	25	22	9	8	< 3	75	20	4	401
	ER 232	85.27	1.18	9.02	0.44	< 0.01	0.07	0.16	0.47	0.95	0.03	97.65	0.19	30	55	< 2	21	5	< 7	10	85	19	4	395
	ER 233	86.12	1.20	8.82	0.64	< 0.01	0.06	0.24	0.10	0.14	0.05	97.45	0.20	< 12	57	< 2	21	14	19	< 3	109	20	5	407
	ER 234	86.63	1.14	9.24	0.54	< 0.01	0.07	0.24	< 0.01	0.21	0.04	98.18	0.20	17	50	< 2	19	11	8	< 3	86	20	2	386
Refractory bricks	ER235	88.39	1.06	7.99	0.52	< 0.01	0.07	0.14	< 0.01	0.11	< 0.01	98.34	0.12	< 12	54	< 2	21	13	19	< 3	95	19	11	348
	ER236	88.81	1.07	8.10	0.53	< 0.01	0.07	0.14	< 0.01	0.12	< 0.01	98.90	0.10	< 12	56	< 2	21	14	17	< 3	95	20	13	363
	ER237	88.39	1.06	7.78	0.58	< 0.01	0.07	0.20	0.07	0.14	0.01	98.38	0.10	19	50	< 2	20	13	21	< 3	106	20	8	361
	ER238	87.90	1.04	7.62	0.57	< 0.01	0.07	0.18	< 0.01	0.12	0.02	97.59	0.07	< 12	42	< 2	20	11	18	< 3	103	20	10	353
	ER239	86.81	1.04	7.59	0.57	< 0.01	0.08	0.18	< 0.01	0.14	< 0.01	96.47	0.08	< 12	54	< 2	20	11	12	< 3	101	19	2	339
	ER240	87.68	1.05	7.59	0.55	< 0.01	0.08	0.57	< 0.01	0.15	0.01	97.74	0.17	< 12	40	< 2	21	11	12	< 3	106	20	12	369
	ER241	87.95	1.06	7.84	0.58	< 0.01	0.08	0.17	< 0.01	0.18	0.01	97.93	0.08	< 12	48	< 2	19	12	28	< 3	103	19	11	346
	ER242	86.40	1.17	8.84	0.60	0.01	0.08	0.29	< 0.01	0.13	0.03	97.62	0.08	28	51	52	22	13	18	< 3	107	21	12	380
Red bricks	ER243	79.82	0.73	10.93	2.81	0.03	0.90	0.93	0.32	1.41	0.05	98.05	0.64	288	71	24	13	39	24	83	97	16	74	248
	ER247	80.90	0.72	8.75	3.37	0.03	0.61	0.40	1.39	2.70	0.03	99.02	0.97	274	60	26	11	22	23	93	73	18	59	472

Table 5
Major oxides and trace element concentrations (XRF) of the unconsolidated samples from the Waldemme Valley (LOI = loss on ignition)

Sample	SiO_2 (wt. %)	TiO_2 (wt. %)	Al_2O_3 (wt. %)	Fe_2O_3 (wt. %)	MnO (wt. %)	MgO (wt. %)	CaO (wt. %)	Na_2O (wt. %)	K_2O (wt. %)	P_2O_5 (wt. %)	Sum (wt.%)	LOI (wt. %)	Ba (ppm)	Cr (ppm)	Cu (ppm)	Nb (ppm)	Ni (ppm)	Pb (ppm)	Rb (ppm)	Sr (ppm)	Y (ppm)	Zn (ppm)	Zr (ppm)
ER 259	95.83	0.23	1.28	0.11	< 0.01	0.20	0.12	3.44	0.46	0.08	101.80	1.50	42	15	8	6	6	10	7	23	20	< 2	471
ER 261	86.49	0.82	8.66	0.86	< 0.01	0.53	0.06	0.97	1.61	0.06	100.17	3.23	118	64	< 2	16	10	12	78	50	18	10	567
ER 265	82.70	0.68	10.76	1.53	< 0.01	0.70	0.48	1.99	1.99	0.04	100.99	4.73	318	71	< 2	14	17	22	103	88	13	40	315
ER 266	78.19	0.65	11.82	3.38	0.01	0.80	0.83	0.55	2.06	0.03	98.42	9.36	394	81	< 2	13	22	25	118	102	13	45	244

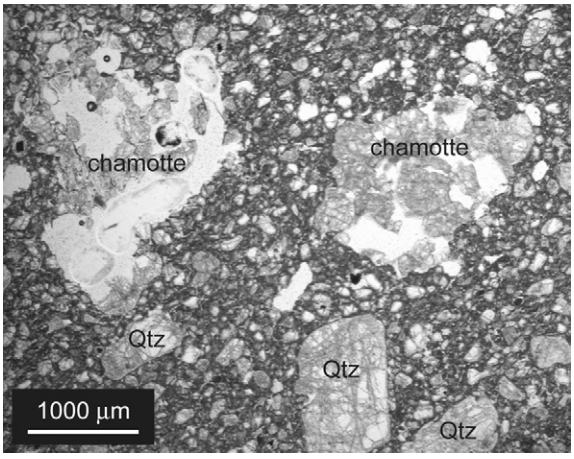

Fig. 6. Image of a crucible sample (ER194) belonging to the petrographic group A, showing fine quartz grains and the as non-plastic inclusions.

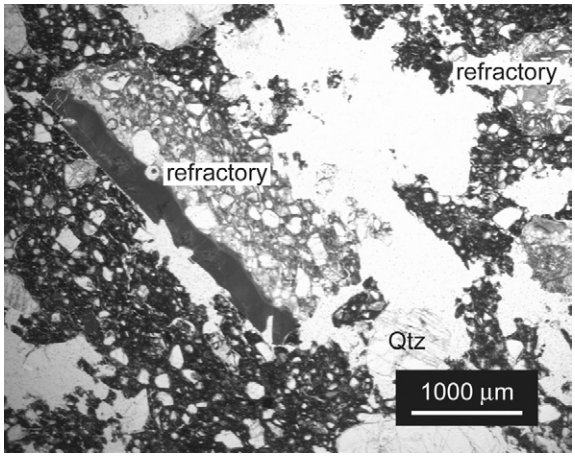

Fig. 8. Image of a red brick (ER243) belonging to the petrographical group B, showing recycled refractory material and coarse quartz grains as temper.

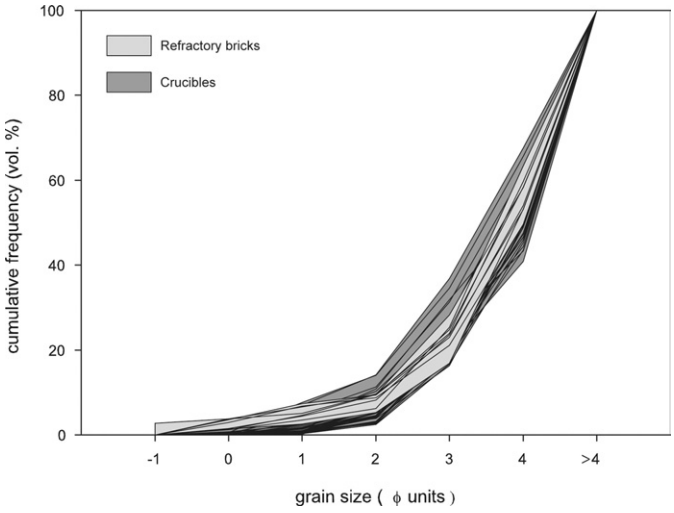

Fig. 7. Image of a refractory brick (ER237) belonging to the petrographical group A, showing *chamotte* clasts and coarse quartz grains as non-plastic inclusions.

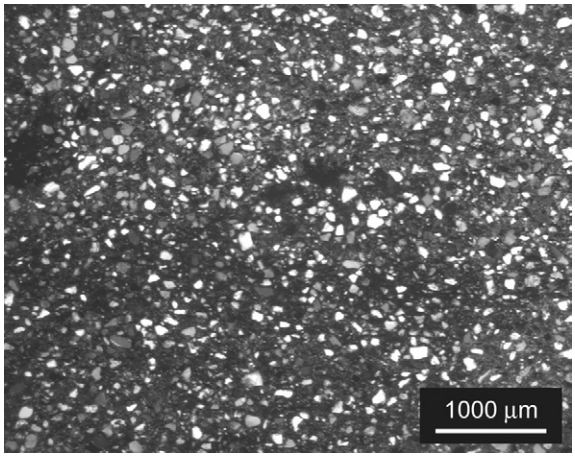

Fig. 9. Image of a red brick with marbled fabric (ER247) belonging to the petrographical group C. showing fine quartz grains as non-plastic inclusions in an iron-rich matrix.

bricks. This demonstrates that the refractory clay was processed in two different manners: the use of clay only for the crucibles and the blending of clay with *chamotte* for the refractory bricks.

The crucible making as well as the reparation of the melting furnace were seasonal activities complementary to glass making [14,15]. Although the same refractory clay was generally used to make crucibles and to line the furnaces, the lifetime of the crucibles was no doubt shorter than that of the furnaces and for this reason the raw materials used might not be the same.

According to Siegwart [3], a high amount of refractory clay and *chamotte* was imported from Germany in 1741. Since this was the last year of activity of the glassworks of Südel, at least the crucible fragments analyzed in this study should have been made with these imported raw materials.

If the hypothesis of a German refractory clay is true, many possible sources may be taken into account. The closest German region to Switzerland is the Black Forest, but it has no good refractory clay deposits [16]. In Vosges and in the Black Forest, as well as in Entlebuch, whilst local quartz sand was exploited to make glass, glassmakers used to import

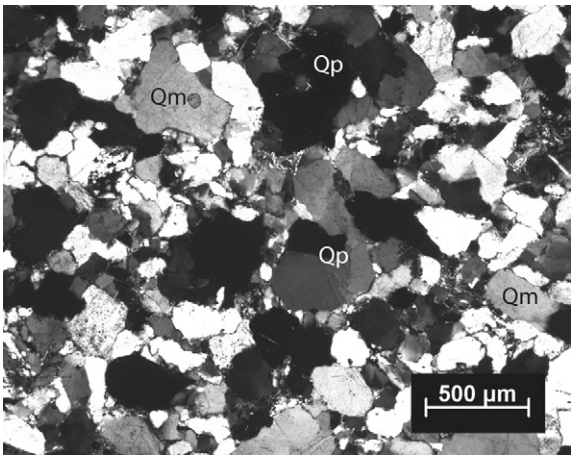

Fig. 10. Few polycrystalline (Qp) quartz surrounded by the prevalent monocrystalline (Qm) quartz in ER258 (Unterer Quarzsandstein).

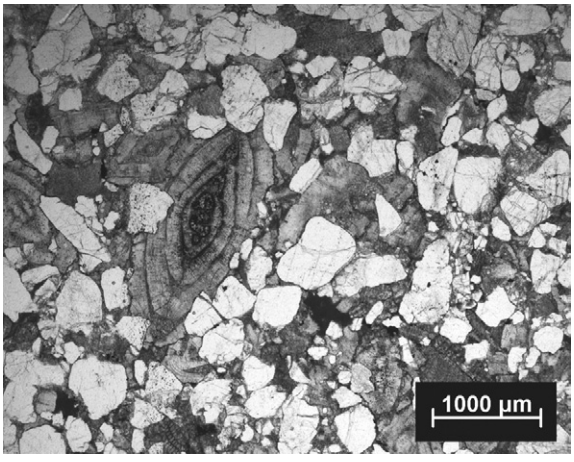

Fig. 11. Bioclasts of nummulites and siliciclastic framework of Complanatakalk (ER257).

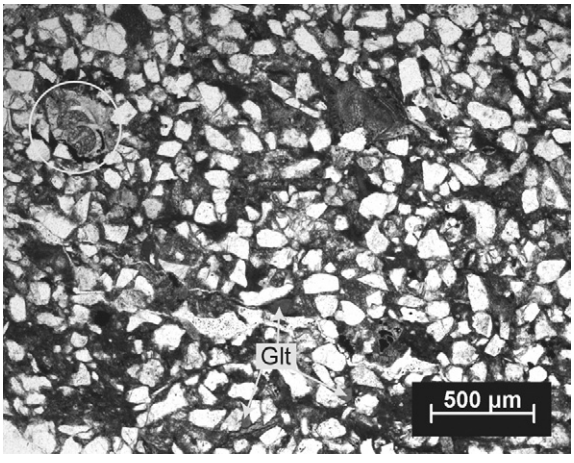

Fig. 12. Bioclasts of foraminifera (circle) and glauconite (Glt) in ER260 (Unterer Quarzsandstein). Micritic cement is present.

the clay to make crucibles and the refractory components of the furnace [17,16,18].

The chemical compositions of six crucibles from different Medieval and post-Medieval glassworks in the Black Forest [16], as well as those of 24 samples of the oval crucibles from the glassworks of "Glaswasen" (15th century, Baden-Württenberg) show Al_2O_3 and Fe_2O_3 percentages higher than those of the crucibles of Südel [19]. Wedepohl [20] reports a kaolinite content of about 50% for the crucibles of the glassworks of Schönbuch (Tübingen). Maus and Jenisch [16] suggest that residual clay of weathered granitic rocks were used for the 13th–15th century samples in the Black Forest. Most recent glassworks are reported to have imported *Kaolinsand* from south-eastern Germany (e.g. Passau, Kalchsreuth and Kelheim) and from north of the Black Forest (e.g. Rastatt, Eisental, Balg, Eisenberg, Worms and Grünstädt) [16,21]. Such kaolinitic clays of different types and quality are still used in the ceramic and the refractory industry [22,23].

Although these deposits may be possible sources for the refractory clay used in Südel, their distance can not be neglected. On the other hand, the Hupper deposits in the Swiss Jura (Fig. 1) may represent a good quality source, closer than those in Germany. The refractory clay, exported in 1634 from Solothurn (eastern border of Swiss Jura) to the glassworks of Rotwasser (Black Forest), which was operated by two members of the Siegwart family, proves that they knew and used the Hupper clayey sand (Sidérolithique Formation) [16]. One century later, the Siegwart glassmaker family managed the glassworks of Südel, but had family members all over the Swiss Jura [14].

The Sidérolithique Formation is a complex geological unit occurring in karstic pockets, or rarely as continuous beds, on the Mesozoic limestones of the Swiss Jura [24–28]. The Hupper sediments form the upper portion of Sidérolithique and are a heterogeneous mixture of quartz sand and clay. However, some outcrops have prevalent quartz sand or clay to be exploited separately. The chemical composition of Hupper varies as a function of clay content. Al_2O_3 concentrations up to 15 wt.% for clay-rich samples were reported by De Quervain [29]. The low alkali and iron content, as well as the variable amount of kaolinite in the Hupper sand, made this sediment a resource for both vitrifiable sand and refractory clay, as evidenced by Eramo [30] on furnace's refractory fragments and the crucibles of the glassworks of Derrière Sairoche (1699–1714) in the Swiss Jura.

The demonstration of a quartz sand trade from Swiss Jura to Südel argues for the possibility that the glass makers imported the refractory clay too, since it is associated with quartz sand in the Hupper deposits [14,28,30,31].

Fifteen variables of the crucibles and the refractory materials of Südel and Derriére Sairoche [8,32] and the refractory clay (Hupper) cropping out in the Swiss Jura [30] were processed by PCA to understand how similar the crucibles and the refractory bricks of these two sites are and whether or not the Hupper can be compatible as a raw material.

The first three principal components (PCs) account for 62.58% of total variance (Table 6). PC1 (35.89%), PC2 (16.50%) and PC3 (10.23%) give at the same time the chemical and textural fingerprint of the different sample groups. The association of the loadings of the variables in each PC gives a

Table 6
PCA: eigenvalues and variance contributions for each component

Component	Eigenvalue	Variance (%)	Cum.Var. (%)
1	5.38	35.89	35.89
2	2.47	16.47	52.36
3	1.53	10.23	62.58
4	1.17	7.79	70.37
5	1.05	7.03	77.40
6	0.89	5.92	83.31
7	0.70	4.66	87.97
8	0.55	3.69	91.66
9	0.45	3.02	94.68
10	0.30	1.98	96.65
11	0.23	1.50	98.15
12	0.15	0.99	99.14
13	0.09	0.60	99.74
14	0.04	0.24	99.97
15	0.00	0.03	100.00

Table 7
PCA: loadings of the first three PCs

	Component		
Variable	1	2	3
SiO_2	–0.855	–0.150	0.095
TiO_2	0.664	–0.563	–0.064
Al_2O_3	0.751	0.098	-0.452
Fe_2O_{3tot}	0.474	0.431	0.108
MgO	0.339	0.660	0.113
CaO	0.217	0.271	0.477
K_2O	0.620	0.465	–0.036
Cr	0.647	0.261	–0.541
Sr	0.615	–0.211	0.504
Zr	0.532	-0.575	0.098
–1–0φ	–0.007	–0.217	0.535
1–2φ	–0.631	0.476	0.208
2–3φ	–0.784	0.302	–0.263
3–4φ	–0.231	–0.631	–0.284
> 4φ	0.855	0.062	0.168

different point of view on the data structure. PC1 features negative loadings of SiO_2, 1–2φ and 2–3φ and positive loadings of the>4φ fraction and of the chemical variables associated with the finest grain-size fraction (Table 7). PC2 shows an inversion of the absolute value in the loadings of variables such as SiO_2, MgO, Al_2O_3, >4φ, 2–3φ and 3–4φ PC3 gives a contribution to the total variance similar to that given by PC2, but is characterized by positive loadings of –1–0φ, CaO and Sr, and by negative loadings of Al_2O_3 and Cr. The score plot on PC1–PC3 shows less correlated data than PC1–PC2 and provides a clearer picture of the data structure (Fig. 13a, b), by eliminating redundancies of information. The component plot PC1–PC2 (Fig. 13c) shows more obvious associations of variables such as Al_2O_3–>4φ and Zr–TiO_2. Both the score plots show an overlapping of the crucibles and the refractory bricks of Südel, slightly differing from those of Derrière Sairoche. As concerns the refractory clay, only some of the Hupper samples are compatible with the archaeological materials. A comparison between Fig. 13b and d reveals that the grain-size variables characterize the crucibles and refractory materials better than the chemical variables. Their data are clustered close to the origin, toward the upper left quadrant (Fig. 13b), where the PC1 loading of SiO_2, 2–3φ and 1–2φ, and the PC3 loading –1 to 0φ are important for the differences observed among the classes of samples.

The overlapping between the crucibles and the refractory materials of Südel shows that they were made with the same raw material and that the *chamotte* added to the clay body of the refractory bricks did not induce chemical variation, an indication that it was obtained firing the same refractory clay. Although the refractory materials of Südel and Derrière Sairoche have similar features, the former were made by adding *chamotte* to the refractory clay, whilst the latter was made with unprocessed refractory clay [30].

Even if PCA established significant similarities between the crucibles and the refractory materials of Südel and some of Hupper samples analyzed by Eramo [30], a German provenance of the clay can not be ruled out definitely.

6.2. Temperature distribution in the melting chamber

The XRD analyses showed that all the refractory fragments and most of the crucible fragments contain quartz, tridymite, cristobalite and mullite, whereas the remaining portion of the crucible fragments lacks tridymite (Table 1). The mullite and cristobalite co-occurrence points to temperatures higher than 1200 °C [33–35], whilst tridymite was formed at the expense of both quartz and cristobalite [36].

As discussed elsewhere [8,32], this phase association is not indicative of a realistic temperature range, due to the instability of tridymite in a pure silica system. Indeed, its formation depends, for a given system, on chemical composition, temperature and reaction time [36,37]. However, since the *d*-spacing of the (101) planes of cristobalite is related to the crystallization temperature [38], its determination can infer the maximum temperature at which the crucibles and the refractory bricks were exposed [8,32]. According to the XRD analyses, $d_{(101)}$ of cristobalite ranges from 0.4053 to 0.4066 nm (± 0.0002) in the crucibles and from 0.4064 to 0.4078 nm (± 0.0002) in the refractory bricks (Table 1).

The box plot in Fig. 14 shows the range and the symmetry of the $d_{(101)}$ values of cristobalite measured in the crucibles and in the refractory bricks. Forty five out of 50 crucible fragments show $d_{(101)}$ of cristobalite comprised between 0.4059 and 0.4063 nm with a skewed distribution towards higher values. Since 27 out of 50 the $d_{(101)}$ of cristobalite of the crucibles fragments equals 0.4059 nm, the median coincides with the 25th and the 10th percentile (Fig. 14). While the two higher outliers follow the trend of the data distribution, the three lower outliers have a different behavior. This kind of data distribution points to a quite homogeneous thermal conditions for the crucibles. The refractory bricks show more dispersed but normally distributed $d_{(101)}$ values (Fig. 14). Therefore, all the $d_{(101)}$ values will be taken into account for the temperature determination, with the exception of the three lower outliers, which will be treated in a different way.

According to the master curve, which relates $d_{(101)}$ of cristobalite and the crystallization temperature proposed by Eramo [32], the temperatures recorded by the crucible samples range

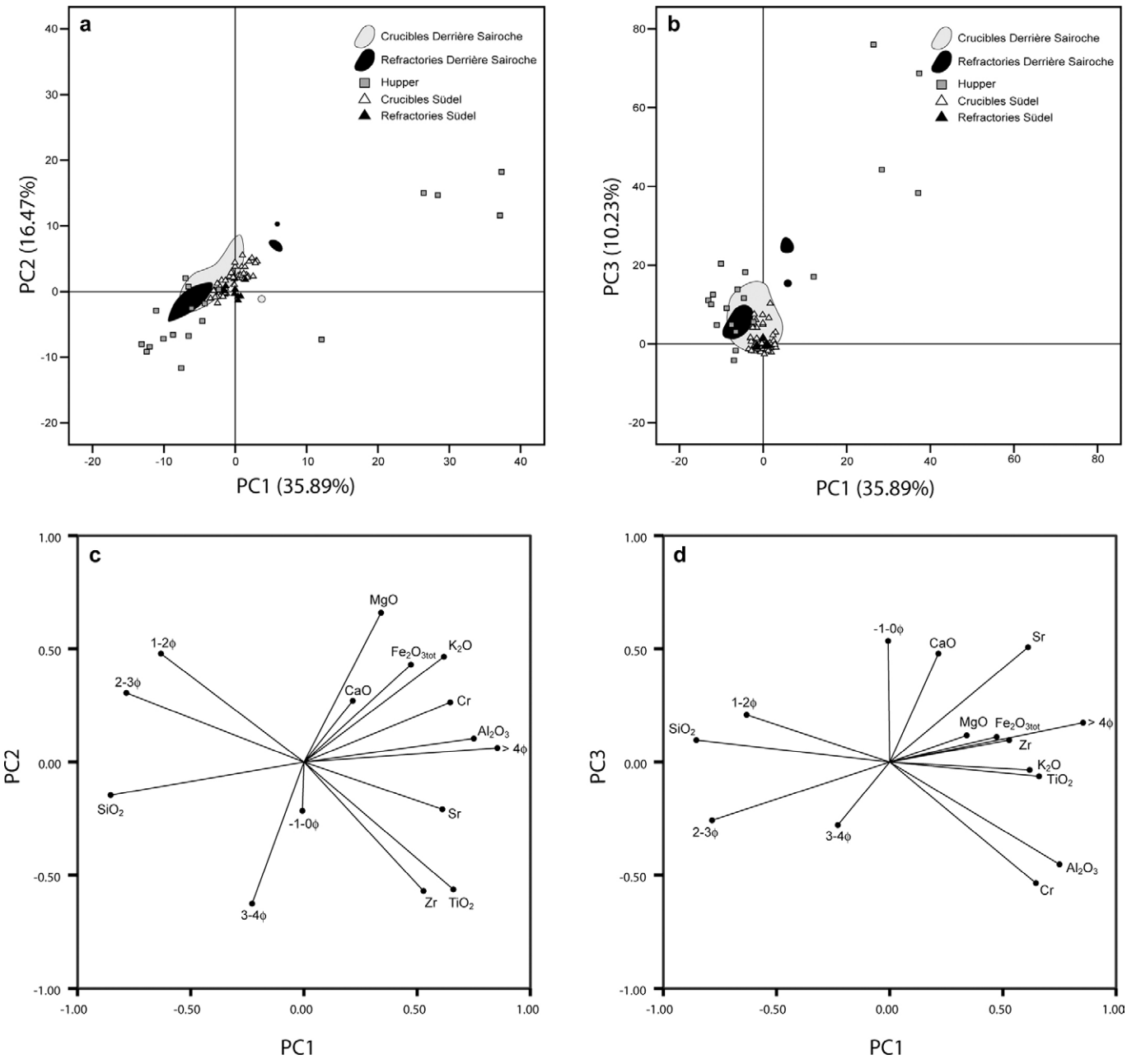

Fig. 13. Score plot PC1–PC2 (a) shows higher correlated data than plot PC1–PC3 (b). The data point of the crucibles and the refractory materials of Derrière Sairoche were substituted by their relative dispersion areas for clarity. The component plot PC1–PC2 (c) shows more obvious associations of variables than those in PC1–PC3 (d).

from 1380° (± 10) and 1500 °C (± 50), whereas those recorded by the refractory bricks range from 1350° (± 10) to 1400 °C (± 10). The refractory bricks from the lower parts of the fire trench were exposed to lower temperatures than those of the higher parts (Fig. 3), although the difference is small. The inferred larger temperature range of the crucibles may be explained by their position between the hottest (flame) and the coldest (glory holes) parts of the melting chamber (Fig. 3). Since the crucible samples are representatives of different portions of the crucible body (Table 1) and show a restricted temperature range, it can be inferred that the temperature on the sieges was quite homogeneous. As shown by Table 1, the color of the crucible body is not necessarily related to the temperature to which it was exposed, but to the atmosphere of the melting chamber [8]. The chromatic differences observed in the restored crucible (Fig. 4) occurred before surface vitrification, when differences in oxygen fugacity throughout the melting chamber could have affected the iron-oxidation state. Although the body color recorded the red-ox conditions during its firing, the occurrence of glass drippings associated to the side, with orange body, exposed to the glory hole demonstrates that the crucible stayed in the same position during both its firing and its use. Thus, the portion of the crucibles exposed to the flame turned to gray or violet, whilst the side exposed to the glory hole turned to yellow. The three samples with the lowest cristobalite $d_{(101)}$ point to temperatures of about

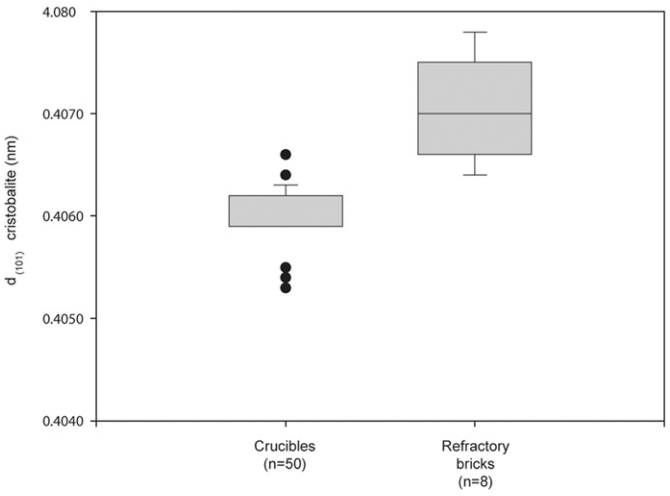

Fig. 14. Box plots of $d_{(101)}$ cristobalite measured in the crucibles and in the refractory bricks of Südel. The median coincide with the 25th and 10th percentile in the box plot of the crucibles. whilst it falls in the interquartile range (gray box) in the box plot of the refractory bricks. The whiskers indicate the range between the 10th and 90th percentile.

1650 °C (± 50) and their gray or gray–violet color suggesting that they were exposed to the flame.

As concerns the red bricks, ER243 (petrographic group B) shows a chromatic zoning from orange to violet in the outermost portion exposed to fire. The absence of illite/muscovite peaks in the XRD spectrum of the violet portion and the presence of hematite suggest temperatures between 1050 and 1100 °C, while the presence of illite/muscovite peaks in the orange portion, as well as the (002)/(110) peak ratio, points to temperatures below 600 °C [39]. Cristobalite and traces of mullite detected in ER243, belong to the refractory temper fragments and can not be used for temperature deductions.

Illite/muscovite were detected in the XRD spectrum of ER247 (group C), a fact that points, in combination with the (002)/(110) peak ratio, as for ER243, to temperatures below 600 °C [39]. This suggests that both bricks were used unfired to build the furnace, because they would have been fired in the range of 800–900 °C in a normal ceramic kiln. The refractory bricks did not show relevant color/fabric differences as the red bricks, which could have been inferred by their unfired use. However, the use of unfired red bricks may indicate that the refractory bricks were used unfired too. The practice of constructing a furnace from unfired bricks is reported in several historical sources [14,15,17]. The firing of all the structure occurred during the preliminary gradual heating of the melting furnace before its regular activity.

Therefore, they recorded the temperatures reached during the use of the melting furnace. All these temperature estimations can be combined in a hypothetic temperature distribution in the melting chamber (Fig. 3).

The temperatures estimated for the melting furnace of Südel are in agreement with those obtained for Derrière Sairoche [8,32]. However, maximum temperatures of about 1650 °C, as in the case of Südel, seem very high. Such flame temperatures are theoretically possible for wood fuel [40] and the presence of the air vents through the sieges may explain these very high flame temperatures, caused by an increase of air rate in the fire trench [41]. Crucible fragments in direct contact with the flame would have recorded higher temperatures as usual.

7. Conclusions

Petrographic, mineralogical and chemical analyses of 50 glass-melting crucibles and 10 fragments of melting furnace lead to an estimation of the temperature distribution in the melting furnace of Südel and to determine the provenance of the raw materials used for the crucibles and the melting furnace. In the melting chamber, temperatures between 1350 and 1500 °C are plausible. However, three samples point to temperatures as high as 1650 °C. Such high temperatures are consistent with measured wood flame temperatures up to 1800 °C [40].

The statistical processing (PCA) at the same time of the chemical and grain-size data gave a chemical and textural fingerprint of the crucibles and refractory bricks, showing that they were made with the same raw material, whilst the petrographic analysis revealed two different processing. Natural clayey sand was used to make the crucibles, whilst the same clayey sand blended with *chamotte*, obtained from the same raw material, was used to make the refractory bricks. The local resources are not compatible as raw materials. Archaeologists hypothesize German provenance of the refractory clay, but suitable deposits are 400–500 km away from Südel. Another provenance is suggested by the fact that the composition of the refractory materials of Südel approaches that of Derrière Sairoche, and that falls in the distribution area of the compositional point of the Swiss Jura Hupper sand compositions. Therefore, the shorter distance compared to German deposits and the existing trade of pure quartz sand from the Swiss Jura to Südel for the colorless glass supports the use of Hupper clayey sand as refractory clay. The red bricks were produced with a local, calcium-poor, clay from the talus, either almost unprocessed (ER247) or tempered with recycled refractory fragments (ER243). The latter confirms a local production of the red bricks. The low temperatures (< 600 °C) recorded by ER247 point to the use of unfired red bricks to build the furnace. Although in the case of the refractory bricks it was not possible to distinguish the thermal effects due to firing from those due to use, the use of unfired red bricks suggest the same practice for them too. This is in agreement with the constructive technique known in literature [14,15,17].

This study provided further evidences of high thermal performances of wood-fed melting furnaces in the pre-industrial period, obtained independently from the liquidus temperature of glass. Although wood fuels have heating values lower than fossil fuels, these results demonstrate that wood pyrotechnology in the pre-industrial period could provide thermal performances comparable to those of coal or peat.

Further investigations on the provenance of the raw materials for the glassworks of Germany, France, Czech Republic and Switzerland will throw light on the circulation of the

refractory clay related to glass making in post-medieval Central Europe.

Acknowledgments

This article is part of a Ph.D. thesis under the direction of Professor M. Maggetti and of Dr. G. Thierrin-Michael (University of Fribourg). The author is indebted to them for their support and constructive criticism. Dr. V. Serneels is kindly acknowledged for the XRF analyses. Thanks are also due to Dr. J. Manser and Dr. E. Nielsen of the Archaeological Survey of Canton Lucerne and to Dr. H. Horat of the Historical Museum of Lucerne for their collaboration.

References

[1] R. Schider, Geologie der Schrattenfluh im Kanton Luzern, Beiträge zur Geologischen Karte der Schweiz 63, Bern, 1913.
[2] H. Horat, Flühli-Glas, Haupt, Stuttgart, Bern, 1986.
[3] L. Siegwart, Jubiläumsschrift zum hundertsten Betriebsjahre der Glashütte Hergiswyl (Nidwalden) 1818–1918, unpublished report, Luzern, 1918.
[4] E. Zaugg, Die schweizerische Glasindustrie, Ph.D, Universität Zürich, Schweiz, 1922.
[5] G. Descoeudres, H. Horat, W. Stöckli, Glashütten des 18, Jahrhunderts Entlebuch Jahrb. Historischen Ges. Luzern 3 (1985) 2–45.
[6] H. Horat, Der Glasschmelzofen des Priesters Theophilus, Haupt, Stuttgart, Bern, 1991.
[7] H.G. Stephan, Glasschmelzgefässe: Grundzüge der Entwicklung von den Anfängen im Alten Orient bis zur Neuzeit, in: P. Steppuhn (Ed.), Glashütten im Gespräch, Berichte und Materialien vom 2 Internationalen Symposium zur archäologischen Erforschung mittelalterlicher und frühneuzeitlicher Glashütten Europas, Verlag Schmidt-Römhild, Lübeck, 2003, pp. 136–162.
[8] G. Eramo, The glass-melting crucibles of Derrière Sairoche (1699–1714 AD, Ct. Bern, Switzerland): a petrological approach, J. Archaeol. Sci. 33 (2006) 440–452.
[9] R. Trümpy, Geology of Switzerland, a guide-book. Part A, Schweizerische Geologische Kommission (Ed.), Wepf and Co., Basel, 1980.
[10] U. Menkveld-Gfeller, Die Bürgen-Fm. und die Klimsenhorn-Fm.: Formelle Definition zweier lithostratigraphischer Einheiten des Eozäns der helvetischen Decken, Eclogae Geol. Helv. 90 (1997) 245–261.
[11] O. Kempf, O.A. Pfiffner, Early Tertiary evolution of the North Alpine Foreland Basin of the Swiss Alps and adjoining areas, Basin Res. 19 (2004) 549–567.
[12] A. von Moos, Kurze Untersuchung der ehemaligen Ausbeutestellen von Glassand in der Umgebung von Flühli (Luzern), Romoos (Luzern) und Küssnacht (Schwyz), Kriegs-Industrie-und Arbeitsamt, Büro für Bergbau, unpublished report, 1942.
[13] G.M. Friedman, Determination of sieve-size distribution from thin-section data for sedimentary petrological studies, J. Geol. 66 (1958) 394–416.
[14] G.J. Michel, Verriers et verreries en Franche-Comté au XVIII^{e} Siècle (2 tomes), Editions ERTI, Paris, 1989.
[15] P. Piganiol, Le verre. Son histoire. Sa technique, Hachette, Paris, 1965.
[16] H. Maus, B. Jenisch, Schwarzwälder Waldglas: Glashütten, Rohmaterial und Produkte der Glasmacherei vom 12.-19, Jahrhundert Alemannisches Jahrb. 1997 (98) (1998) 325–524.
[17] V. Brumm, Un pays du verre et du cristal les Vosges du nord au siecle des lumieres, mémoire de maîtrise d'histoire réalisé par Véronique Brumm, Université des sciences humaines de Strasbourg, Strasbourg, France, 1997.
[18] B. Scholz, Kirn, Early Nineteenth Century Glass Technology in Austria and Germany (translated by M. Cable), The Society of Glass Technology, Sheffield, 2004.
[19] B. Watzke, Materialwissenschaftliche Untersuchungen von Produktionseinrichtungen und Produkten der spätmittelalterlichen Glashütte Schönbuch, Master thesis, Universität Würzburg, Germany, 2004.
[20] K.H. Wedepohl, Glas in Antike und Mittelalter, E. Schweizerbart'sche Verlagsbuchhandlung, Stuttgart, 2003 (Nägele u. Obermiller).
[21] P. Wagenplast, Die Rohstoffe der baden-württembergischen Glashütten, Aufschluss 49 (1998) 286–292.
[22] K. Jasmund, G. Lagaly, Tonminarale und Tone, Steinkopff Verlag, Darmstadt, 1993.
[23] R. Walter, Geologie von Mitteleuropa, E. Schweizerbart'sche Verlagsbuchhandlung, Stuttgart, 1995 (Nägele u. Obermiller).
[24] E. Fleury, Le sidérolithique suisse, Mémoires de la Société fribourgeoise de Sciences naturelles 6 (1909) 1–260.
[25] E. Schlaich, Geologische Beschreibung der Gegend von Court im Berner Jura : mit Berücksichtigung der Molassebildungen, Beiträge zur geologischen Karte der Schweiz 26 (1934) 1–41.
[26] A. von Moos, Über Vorkommen und Abbau von Giessereiformstoffen in der Schweiz, Eclogae Geol. Helv. 34 (1941) 229–240.
[27] D. Aubert, L'évolution du relief jurassien, Eclogae Geol. Helv. 68 (1975) 1–64.
[28] U. Pfirter, Feuille 1106, Moutier. Atlas géologique Suisse 1:25.000, Notice explicatives 96 (1997).
[29] F. De Quervain, Die nutzbaren Gesteine der Schweiz, Kümmerly and Frey, Geographischer Verlag, Bern, 1969.
[30] G. Eramo, Pre-industrial glassmaking in Swiss Jura: the refractory earth for the glassworks of Derrière Sairoche (Ct. Bern, 1699–1714), in: M. Maggetti, B. Messiga (Eds.), Geomaterials in Cultural Heritage, Special Publications, Geological Society of London 257, London, 2006, pp. 187–199.
[31] G. Amweg, Les Arts dans le Jura bernois et à Bienne, Tome II, Arts appliqués, Porrentruy, 1941.
[32] G. Eramo, The melting furnace of the Derrière Sairoche glassworks (Court, Swiss Jura): heat-induced mineralogical transformations and their technological signification, Archaeometry 47 (2005) 571–592.
[33] M. Bellotto, A. Gualtieri, G. Artioli, S.M. Clark, Kinetic study of the Kaolinite–Mullite reaction sequence. Part I, Kaolinite Dehydroxylation Phys. Chem. Miner. 22 (1995) 207–214.
[34] M. Bellotto, A. Gualtieri, G. Artioli, S.M. Clark, Kinetic study of the Kaolinite–Mullite reaction sequence. Part II, Mullite Formation Phys. Chem. Miner. 22 (1995) 215–222.
[35] S. Lee, Y.J. Kim, H. Moon, Phase transformation sequence from kaolinite to mullite investigated by energy-filtering transmission electron microscope, J. Am. Ceram. Soc. 43 (1999) 2841–2848.
[36] S.J. Stevens, R.J. Hand, J.H. Sharp, Polymorphism of silica, J. Mater. Sci. 32 (1997) 2929–2935.
[37] S.B. Holmquist, Conversion of quartz to tridymite, J. Am. Ceram. Soc. 44 (1961) 82–86.
[38] A.G. Verduch, Kinetics of cristobalite formation from silicic acid, J. Am. Ceram. Soc. 41 (1958) 427–432.
[39] M. Maggetti, Phase analysis and its significance for technology and origin, in: J.S. Olin, A.D. Franklin (Eds.), Archaeological Ceramics, Smithsonian Institution Press, Washington, 1982, pp. 121–133.
[40] D.A. Tillman, Energy generation from wood, in: A. Schniewind (Ed.), Concise Encyclopedia of Wood and Wood-based Materials, Pergamon press, Oxford, 1989, pp. 102–105.
[41] J.E. Rehder, The Mastery and Uses of Fire in Antiquity, McGill-Queen's University Press, Montreal, 2000.